Comparison of Antenna Measurement Facilities with the DTU-ESA 12 GHz Validation Standard Antenna within the EU Antenna Centre of Excellence

Pivnenko, Sergey; Pallesen, Janus Engberg; Breinbjerg, Olav; Castaner, Manuel Sierra; Almena, Pablo Caballero; Portas, Cristian Martinez; Sanmartin, Jose Luis Besada; Romeu, Jordi; Blanch, Sebastian; Gonzalez-Arbesu, Jose M.; Sabatier, Christian; Calderone, Alain; Portier, Gerard; Eriksson, Håkan; Zackrisson, Jan

Published in:
I E E E Transactions on Antennas and Propagation

Link to article, DOI:
10.1109/TAP.2009.2021934

Publication date:
2009

Document Version
Publisher's PDF, also known as Version of record

Comparison of Antenna Measurement Facilities With the DTU-ESA 12 GHz Validation Standard Antenna Within the EU Antenna Centre of Excellence

Sergey Pivnenko, *Member, IEEE*, Janus E. Pallesen, Olav Breinbjerg, *Member, IEEE*, Manuel Sierra Castañer, *Member, IEEE*, Pablo Caballero Almena, Cristian Martínez Portas, José Luis Besada Sanmartín, Jordi Romeu, Sebastian Blanch, *Member, IEEE*, José M. González-Arbesú, Christian Sabatier, *Member, IEEE*, Alain Calderone, Gérard Portier, Håkan Eriksson, *Member, IEEE*, and Jan Zackrisson, *Member, IEEE*

***Abstract*—The primary objective of many antenna measurement facilities is to provide a specified high accuracy of the measured data. The validation of an antenna measurement facility is the process of proving that such a specified accuracy can be achieved. Since this constitutes a very challenging task, antenna measurement accuracy has been the subject of much research over many years and a range of useful measures have been introduced. Facility comparisons, together with antenna standards, error budgets, facility accreditations, and measurement procedure standards, constitute an effective measure towards facility validations. This paper documents the results of a comparison between 8 European antenna measurement facilities with a specially designed reference antenna, the DTU-ESA 12 GHz Validation Standard Antenna (VAST-12). The electrical and mechanical properties of the VAST-12 antenna are presented and its three different coordinate systems are defined. The primary objective of the comparison is to obtain experience and results that can serve to develop standards for validation of antenna measurement facilities. The paper focuses on the comparison of the radiation pattern and presents not only the measurement data obtained at the facilities, but also investigates several procedures for comparing these data. This includes various definitions of pattern difference and statistical measures as well as a reference pattern. The comparison took place in 2004–2005 as part of the European Union network of excellence called *ACE—Antenna Centre of Excellence*.**

***Index Terms*—Antenna measurements, antennas, facility comparison.**

I. Introduction

ANTENNA measurements constitute an indispensable part of the development, approval, or commissioning of any wireless system. Though the accuracy and efficiency of computational tools are ever increasing, stringent specifications and/or high complexity necessitate that the characterization of most antennas be achieved by way of measurements. This is true for analysis and synthesis in the development of antennas, for verification in the approval of antennas, and for calibration in the commissioning of antennas. The importance of antenna measurements increases with the ongoing growth of wireless technologies, and it is reflected in expanding research and development activities as well as numerous new antenna measurement facilities being established.

The primary objective of many antenna measurement facilities is to provide a specified high accuracy of the measured data. The validation of an antenna measurement facility is the process of proving that such a specified accuracy can be achieved. However, the determination of antenna measurement accuracy is a very challenging task for several reasons. First, the true data for any real antenna is always unknown. Second, there are several different antenna measurement techniques and these all possess different sources of inaccuracy. Third, for the individual antenna measurement technique there are several different procedures for its practical implementation, and these procedures again possess different sources of inaccuracy. Fourth, for different antennas, or for different parameters of the same antenna, there are also different sources of inaccuracy, e.g., the measurement of a wide beam antenna is influenced more by ground and wall reflections than the measurement of a narrow beam antenna. In consequence hereof, antenna measurement accuracy has been the subject of much research over many years and a range of useful measures have been introduced, e.g., antenna standards, error budgets, facility accreditations, facility comparisons, and measurement procedure standards. However, because of either limited scope or limited maturity of such measures, as will be discussed below, there is not yet a generally accepted standard for validation of antenna measurement facilities. Each of the above-mentioned measures can contribute in part to the validation. The use of antenna standards, reference antennas with properties known to a high accuracy, obviously provides information on the measurement accuracy. However, today there are very few such generally accepted antenna standards. One example is the DTU-ESA Standard Gain Horns housed at the DTU-ESA Spherical Near-Field Antenna Test Facility at the Technical University of Denmark. The use of error budgets primarily provides information on the precision of an-

Manuscript received January 13, 2009. Current version published July 09, 2009. This work was supported by the EU/ACE.

S. Pivnenko and O. Breinbjerg are with the Technical University of Denmark, DK-2800 Kgs. Lyngby, Denmark (e-mail: sp@elektro.dtu.dk).

J. E. Pallesen was with the Technical University of Denmark, DK-2800 Kgs. Lyngby, Denmark. He is now with Interactive Sports Games, 2950 Vedbæk, Denmark.

M. S. Castañer, P. C. Almena, C. M. Portas, and J. L. B. Sanmartín are with the Technical University of Madrid, 28040 Madrid, Spain.

J. Romeu, S. Blanch, and J. M. González-Arbesú are with the Technical University of Catalonia, E-08028 Barcelona, Spain.

C. Sabatier, A. Calderone, and G. Portier are with France Telecom Research and Development, RESA/FACE, 06320 La Turbie, France.

H. Eriksson is with Saab Microwave Systems AB (formerly Ericsson Microwave Systems AB), SE-431 84 Mölndal, Sweden.

J. Zackrisson is with RUAG Aerospace Sweden AB (formerly Saab Ericsson Space AB), SE-405 15 Göteborg, Sweden.

Digital Object Identifier 10.1109/TAP.2009.2021934

tenna measurements, but together with the rigorous theoretical foundation of, e.g., near-field techniques, the error budget also gives information on the accuracy of such antenna measurement techniques. It is noted here that the term precision refers to the quality of the measurement process, while the term accuracy refers to the quality of the measurement result. Though several suggestions have been reported [1]–[3], there is no generally accepted standard for setting up error budgets. The formal accreditations that can be obtained from several organizations will probably become of more significance in the future, but at present it would appear that the reputation of a measurement facility in the antenna community is of much more importance. The use of measurement procedure standards of course contributes to ensuring the measurement accuracy, but for many measurement techniques, e.g., all near-field techniques, there are not yet such standards available.

Facility comparisons constitute an effective measure towards facility validations and a number of comparisons have previously been conducted. In 1988, Lemanczyk and Larsen [4] reported on two comparisons each involving three facilities. These comparisons concerned radiation pattern, directivity, and gain of a 12 GHz reflector antenna, which was available for the comparisons though not specially designed for this purpose and thus possessing shortcomings with regard to mechanical stability and well-defined coordinate systems. In 1996 Stubenrauch *et al.* [5] reported a comparison involving seven facilities. This comparison concerned on-axis gain and polarization, at three frequencies, of two commercially available and nominally identical X-band standard gain horns. Another comparison of on-axis gain of two significantly different horns at three frequencies in the Ka-band involving five national metrology laboratories has been reported in [6]. Furthermore, a number of smaller comparisons, typically involving just two facilities, have been reported in the literature [7]–[12]. The variety of these facility comparisons reflects the fact that different antenna parameters may require different types of comparisons. In 1995 Lemanczyk [13] gave a thorough overview of the status of European standards for antennas and laboratories and emphasized the need for specially designed reference antennas to be used in facility comparisons.

The purpose of the present work is to conduct a systematic comparison of several antenna measurement facilities, based upon different measurement techniques and procedures, by the use of a specially designed reference antenna, the DTU-ESA 12 GHz Validation Standard Antenna; in short, the VAST-12 antenna. This comparison includes first the measurement campaign to obtain the measurement results at the participating facilities, and second an investigation of several procedures for comparing these results. The primary objective of the comparison is to obtain experience and results that can serve to develop standards for validation of antenna measurement facilities. The secondary objective is to provide each participating facility with an opportunity to benchmark its performance relative to that of other facilities.

The comparison took place in 2004–2005 as part of the activities in the European Union (EU) network of excellence called *ACE—Antenna Centre of Excellence* [14] and a total of six institutions with eight different antenna measurement facilities participated in the comparison. These were France Telecom R&D, RUAG Aerospace Sweden, Saab Microwave Systems, the Technical University of Catalonia, the Technical University of Denmark, and the Technical University of Madrid. The facilities were one far-field range, two compact ranges, one planar near-field range, and four spherical near-field ranges. The DTU-ESA Spherical Near-Field Antenna Test Facility at the Technical University of Denmark served as the coordinator of the comparison. An ACE report documenting the comparison was issued in December 2005 [15]; it is also available from [14]. Some first results of the comparison campaign were presented in [16].

This paper is organized as follows: Section II describes the VAST-12 antenna. The electrical and mechanical properties of this antenna are presented and its three different coordinate systems are defined. Section III describes the measurement campaign, which took place from May 2004 to April 2005 with the first and last measurements both conducted at the Technical University of Denmark. Section IV contains a discussion and investigation of several different procedures for comparing the measured data. This includes various definitions for the difference between two patterns and possible use of so-called noise and pattern weighting functions in these definitions. Also, various statistical measures are employed. Furthermore, the issue of a reference pattern, formed from the patterns obtained at the different facilities, is discussed. Section V then describes the results from the campaign and presents specific results for two representative two-facility comparisons among the many such comparisons that can be formed from the obtained measurement results. Finally, in Section VI it is concluded how this comparison can be used in the development of standards for validation of antenna measurement facilities.

II. DTU-ESA 12 GHz Validation Standard Antenna

The DTU-ESA 12 GHz Validation Standard Antenna (VAST-12) was designed and manufactured at the Technical University of Denmark in 1992 for the European Space Agency (ESA) [17]–[20]. This antenna was designed to serve as a reference antenna for the purpose of comparison and validation of antenna measurement facilities. The VAST-12 antenna is shown in Fig. 1. A number of particular features, which makes this antenna very suitable for the above purpose, can be noted. The antenna is an offset shaped reflector with a circular aperture fed by a conical corrugated horn with a polarizer. The polarizer is capable of shifting the polarization between circular and linear. In this comparison the antenna is operated with linear polarization. This configuration provides a complex pattern with low side lobes and a high ellipticity of the main beam, and thus makes the VAST-12 antenna a challenge to characterize through measurements. The mechanical construction of the VAST-12 antenna is based on a light-weight carbon fiber reinforced polymer support structure (CFRP), making the antenna structure mechanically and thermally very stable. This makes it very suitable for use in comparisons, where different mechanical mountings are used.

For proper comparison of measurement results of an antenna obtained at different antenna measurement facilities, it is important that the results are reported in a clearly defined coordinate system. For the VAST-12 antenna 3 separate coordinate systems

Fig. 1. The DTU-ESA 12 GHz VAST-12.

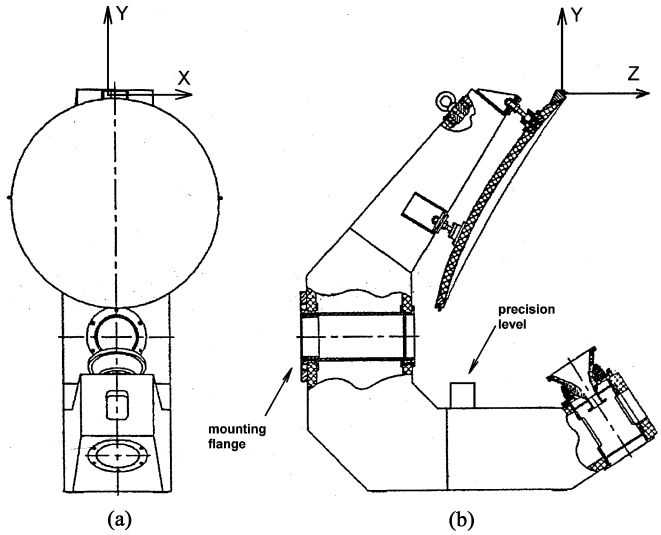

Fig. 2. Front view (left) and side view (right) of the VAST-12 antenna showing its optical coordinate system defined by the mirror cube located on the top rim of the reflector.

are defined in order to ensure that any facility can employ at least one of these [21].

A. The Optical Coordinate System

The optical coordinate system is defined by a mirror cube mounted on the top rim of the reflector (visible in Fig. 1 and shown in Fig. 2). This coordinate system is a normal right hand coordinate system with $\hat{x}$, $\hat{y}$, and $\hat{z}$ unit vectors coinciding with the normal unit vectors of 3 faces of the mirror cube. Due to the mounting of the mirror cube, the positive x axis is not available. Thus the $-x$ axis must be used for alignment purposes.

A test facility has the choice of mechanically aligning the antenna with respect to the mirror cube directly in the facility to make the optical coordinate system coincide with the measurement coordinate system. This requires proper alignment tools such as a theodolite or tracking laser and an adjustable test antenna mounting head. Alternatively, the antenna can be measured in an arbitrary measurement coordinate system and the measurement results then transformed into the optical coordinate system making use of, e.g., the Euler angles defining the optical coordinate system with respect to the measurement coordinate system. For a treatment of rotation of spherical waves and Euler angles, please see [1].

B. The Mechanical Coordinate System

For the mechanical coordinate system, the z-axis is defined by the rotation axis of the measurement system, and thus the xy-plane nominally coincides with the mounting flange on the back side of the VAST-12 antenna. The x axis $(\phi = 0^\circ)$ is then defined to be horizontal with a precision level placed in the specified place on the feed support arm and leveled, as shown in Fig. 2.

C. The Electrical Coordinate System

For the electrical coordinate system, the z axis is defined by the direction of maximum directivity. In order to find the maximum, the direction perpendicular to the mounting flange can be taken as a starting point as the maximum is very close to this. In this process, the antenna can be assumed primarily vertically-polarized, i.e., the electric field vector is primarily in the zy plane of the optical coordinate system, see Fig. 2. Care should be exercised here as the VAST-12 has a rather flat top in the main beam.

A minimum signal is then obtained from the orthogonal port of the range probe by rotating the probe around its symmetry axis or by rotating the antenna around the above defined z axis. This defines the x-axis. This procedure assumes a very good linearly polarized probe.

III. Measurement Campaign

The comparison took place during 2004 and 2005, with the measurement campaign itself from May 2004 to April 2005, ending in December 2005 [15]. A total number of 8 facilities participated and provided measurement results. The participating facilities are listed in Table I, and these include spherical near-field (SNF), planar near-field (PNF), far-field (FF), and compact range (CR) facilities. A description of the specifications and capabilities of each facility is available at the ACE Virtual Centre of Excellence [14].

During the preparation of the measurement campaign a verification test plan (VTP) was adopted. The purpose of the VTP was to ensure that the measurements at each facility were conducted according to standard definitions for the antenna parameters of interest, that the necessary data was documented for each measurement, and that the measurement results were supplied in a

TABLE I
LIST OF PARTICIPATING FACILITIES

Participant	Facility Acronym	Facility Type
Saab Microwave Systems	SMW	CR
France Telecom R&D	FTRD	FF
RUAG Aerospace Sweden	RSE	SNF
Technical University of Catalonia	UPC	SNF
Technical University of Denmark	DTU1, DTU2	SNF
Technical University of Madrid	UPM1	SNF
Technical University of Madrid	UPM2	PNF
Technical University of Madrid	UPM3	CR

documented, and agreed upon, format. As such, the VTP was a document containing a list of parameters such as the pattern cuts to be supplied, the coordinate systems to be used, and the data format to be used. Each participant would then indicate in this document what measurements had been done and in which coordinate system and format the results of these were supplied. Furthermore, a user data package (UDP) was adopted and included with the VAST-12 antenna. The UDP consisted of a number of documents including a VAST-12 antenna Storage and Handling Manual, a VAST-12 antenna Visual Inspection and Damage Status Report, a description of the VAST-12 antenna mechanical and electrical interface, and a time schedule for the measurement campaign. The VTP and UDP were adopted from [21], but modified for the purpose of the present campaign.

In the VTP, it was requested that the following quantities were supplied: co- and cross-polar directivity in the four main planes, $\phi = 0°$, 45°, 90°, 135°, peak directivity, peak gain, axial ratio, tilt angle, and peak location.

Throughout the comparison several meetings were held between the participants. This ensured a well defined and commonly agreed execution of the campaign, and enabled fruitful discussions of the results at a later stage.

IV. PATTERN COMPARISON STRATEGY

The measured patterns are considered in the far-field region and, when suppressing a time dependence of $e^{j\omega t}$, it is thus possible to express the radiated electric field $\mathbf{E}(r,\theta,\phi)$ as

$$\mathbf{E}(r,\theta,\phi) = V_0 \frac{e^{-jkr}}{r}\mathbf{F}(\theta,\phi) \tag{1}$$

where $\mathbf{F}(\theta,\phi)$ is the far-field pattern function and V_0 is an amplitude constant. (r,θ,ϕ) are the spherical coordinates of the observation point. The amplitude constant V_0 is defined such that the co-polar component of $\mathbf{F}(\theta,\phi)$ has a magnitude in the interval $[0,1]$, when using Ludwig's third definition for the co- and cross-polar components [22]

$$\mathbf{F}(\theta,\phi) = \hat{e}_{co}F_{co}(\theta,\phi) + \hat{e}_{cx}F_{cx}(\theta,\phi) \tag{2}$$

where $\hat{e}_{co}$ is the co-polar unit vector and $\hat{e}_{cx}$ is the cross-polar unit vector. $F_{co}(\theta,\phi)$ and $F_{cx}(\theta,\phi)$ are the co- and cross-polarized components of the pattern function, respectively. The co- and cross-polar unit vectors are given as [1]

$$\hat{e}_{co} = \hat{\theta}\cos(\phi-\phi_0) - \hat{\phi}\sin(\phi-\phi_0) \tag{3}$$
$$\hat{e}_{cx} = \hat{\theta}\sin(\phi-\phi_0) + \hat{\phi}\cos(\phi-\phi_0) \tag{4}$$

with $\phi_0 = 90°$; hence $\hat{e}_{co} = \hat{y}$ and $\hat{e}_{cx} = -\hat{x}$ at $\theta = 0°$.

Since only the magnitude of the complex co- and cross-polar components of the pattern function will be considered in the following, this will be denoted by $f(\theta,\phi)$ such that

$$f(\theta,\phi) = |F(\theta,\phi)| \tag{5}$$

where $f(\theta,\phi)$ and $F(\theta,\phi)$ refer to either the co- or the cross-polar component of the pattern function.

A. Individual Comparisons and Reference Comparisons

Comparisons of the radiation patterns can be performed in essentially two different ways. Each measured pattern can be compared against any other measured pattern in so-called individual comparisons, or it can be compared against a reference pattern.

Individual comparisons between all the measured patterns give a large amount of results. Such an investigation allows for considering both statistical deviations between patterns from different facilities and an identification of specific differences. An analysis of the observed differences may serve to identify the sources of these.

Comparisons of each measured pattern to a common reference pattern reduces the number of comparisons relative to individual comparisons and, in addition to the above, also allows a benchmarking. The reference pattern must be of the highest achievable accuracy, and comparisons against this thus allow assessing the accuracy of the individual facilities. Obviously, there is no generally good definition of a reference pattern, but there are several ways of constructing this from the available measured patterns. One pattern with the best accuracy estimate could be chosen as the reference or an average of all or some of the available patterns could form the reference. A good definition of a reference pattern would be based on a weighted average of all the available patterns, with the weights based on the accuracy estimates of each facility. This obviously requires that the accuracy estimates be made according to the same procedure, and in case the accuracy estimates are not available, this definition of the reference pattern is of course not practical. However, regardless of how the reference pattern is defined, an accuracy estimate for this must be provided, and the level of the accuracy will obviously influence the conclusions of the comparisons.

B. Pattern Differences

When presenting radiation patterns graphically the magnitude of the pattern is usually given in a logarithmic scale. Hence, when comparing patterns for the same antenna from two separate facilities a natural and often used procedure is to present these logarithmically in a single plot and subsequently compare them through visual inspection. This suggests that a good way to examine the difference between patterns is to take the difference of the patterns in logarithmic scale. Alternatively, the patterns can be considered on a linear scale and a difference formed from these. Furthermore, in each case a weight can be employed for the difference. A total of four definitions of the difference between patterns are considered below, and exemplified for two particular measurement results, DTU1 and DTU2 as presented in Fig. 3. These four differences include, as special cases, all of the most obvious differences that could be employed, and though they basically represent the same informa-

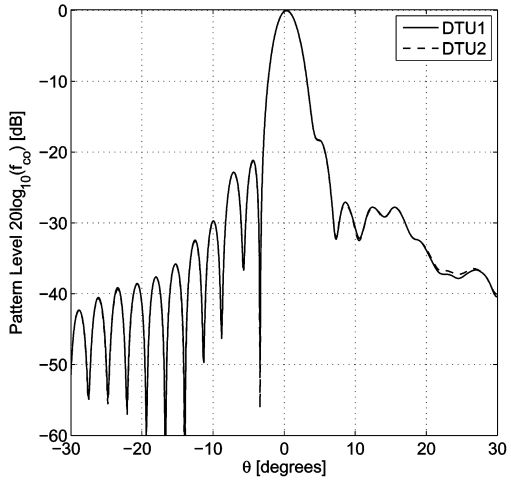

Fig. 3. Magnitude of the co-polar component of the DTU1 and DTU2 patterns in the optical coordinate system for $\phi = 90°$.

tion, they behave in quite different manners. It is noted that while the considerations presented here are focused on the differences in particular pattern cuts, the differences may as well be calculated for the full patterns.

1) Logarithmic Difference: The logarithmic difference is defined as the difference of the magnitudes of the two patterns in logarithmic scale

$$\Delta_{log}(\theta,\phi) = 20\log_{10} f_1(\theta,\phi) - 20\log_{10} f_2(\theta,\phi) \quad (6)$$

where $f_1(\theta,\phi)$ and $f_2(\theta,\phi)$ are the magnitudes of the considered component of the two pattern functions. The logarithmic difference provides an intuitively clear measure for the difference between the patterns as it directly expresses the visible difference between the patterns as seen in Fig. 3. The logarithmic difference is a relative measure, and it is thus small, when the difference between the patterns $f_1(\theta,\phi)$ and $f_2(\theta,\phi)$ (in linear scale) is small relative to the level of the patterns, and large, when the difference is large relative to the level of the patterns. This typically occurs in the main beam region and in minima, respectively. This behavior is clearly visible in Fig. 4(a), where the difference is low in the main-lobe region while having large spikes at pattern nulls (cf. Fig. 3). In particular at the locations of the first, fifth, and sixth null in the patterns, large spikes are visible. These spikes are particularly interesting as they are characterized by a sudden change of sign. This behavior is indicative of a slight shift of the nulls of the two patterns at these locations such that the patterns cross at a very low level and the difference hence changes sign very abruptly. In Fig. 3, a significant difference between the patterns is noticeable in the region around $\theta = 22°$. This difference, which is at a relatively high pattern level, is also noticeable in the logarithmic difference in Fig. 4(a).

2) Weighted Logarithmic Difference: The weighted logarithmic difference is introduced in order to facilitate a weighting of the logarithmic difference according to some predefined criteria. One such criterion could be to de-emphasize the large spikes of the logarithmic difference, which are present near the nulls of the patterns. Other criteria can be set, and further discussion of these and some associated weighting functions will be discussed in Section IV-D. The weighted logarithmic difference is defined as

$$\Delta_{w,\log}(\theta,\phi) = W_{\log}\Delta_{\log}(\theta,\phi) \quad (7)$$

where $W_{\log}$ is the weighting function, which generally can depend on the two pattern functions $\mathbf{F}_1(\theta,\phi)$ and $\mathbf{F}_2(\theta,\phi)$. A particular weighting function that will de-emphasize the difference at low pattern levels is $W_{\log} = (f_1(\theta,\phi))^{\beta}$, where the value of β can be chosen. Using this definition of the weighting function with $\beta = 0.5$ the weighted logarithmic difference will behave as shown in Fig. 4(b). As it is clearly seen from a comparison of this figure to Fig. 4(a), the large spikes of the logarithmic difference are greatly reduced. Furthermore, the relative level of the difference in the main lobe region has increased, and the difference between the patterns in the region around $\theta = 22°$ remains clearly visible. A tradeoff for introducing the weighting of the logarithmic difference is an added complexity in the direct interpretation of what the difference expresses, as this requires an understanding of the weighting function and its influence.

3) Linear Difference: The linear difference is calculated as the difference between the patterns in a linear scale. This difference will generally be large where the pattern level is large and low where the pattern level is low. Hence, this difference has an opposite behavior compared to the logarithmic difference. An expression for the linear difference is

$$\Delta_{\text{lin}}(\theta,\phi) = f_1(\theta,\phi) - f_2(\theta,\phi). \quad (8)$$

In Fig. 4(c) it is seen that the linear difference does indeed become relatively large at high pattern levels and low at low pattern levels.

It can be shown that an equivalent extraneous error signal E_s often used in the literature for pattern comparison (see, e.g., [12]) represents the linear difference in a logarithmic scale

$$20\log_{10} E_s = 20\log_{10}\left(\frac{|\Delta_{\text{lin}}(\theta,\phi)|}{2}\right). \quad (9)$$

4) Weighted Linear Difference: It may be of interest to emphasize or de-emphasize particular characteristics of the linear difference. Based on the linear difference the weighted linear difference is defined as

$$\Delta_{w,lin}(\theta,\phi) = W_{\text{lin}}\Delta_{\text{lin}}(\theta,\phi) \quad (10)$$

where W_{lin} is the weighting function which generally can depend on the two pattern functions $\mathbf{F}_1(\theta,\phi)$ and $\mathbf{F}_2(\theta,\phi)$. If the weighting function is chosen as $W_{\text{lin}} = (f_1(\theta,\phi))^{-1}$ the weighted linear difference becomes the relative difference between the patterns. Hence, in this case the weighted linear difference is approximately proportional to the logarithmic difference, which is also clearly visible from the plot of the weighted linear difference, see Fig. 4(d) and compare with Fig. 4(a).

C. Measures of Merit

In order to quantify the difference between two patterns in general, or a particular characteristic of the difference, various measures of merit can be considered.

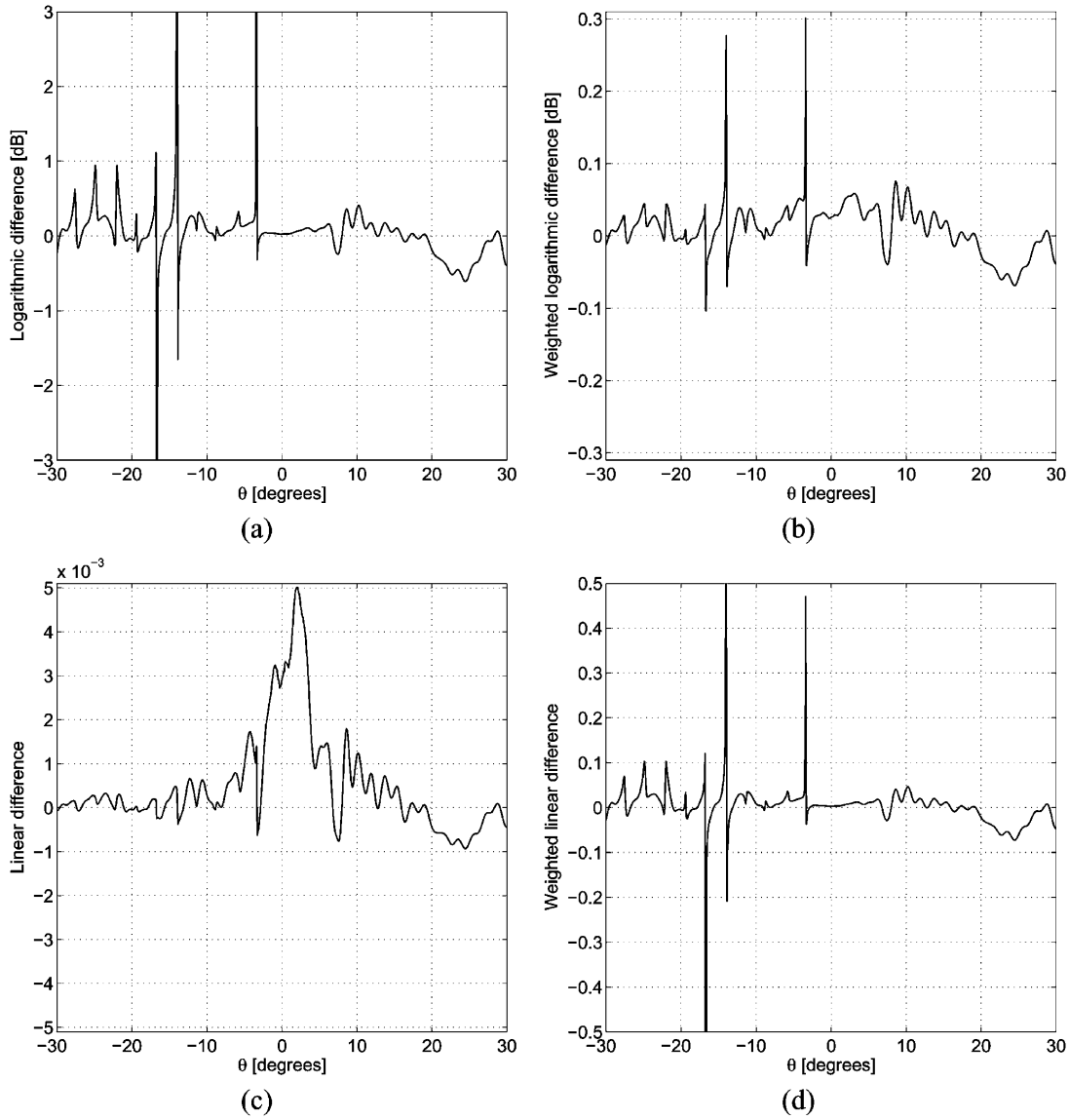

Fig. 4. Illustrations of the defined differences. (a) shows the logarithmic difference, (b) the weighted logarithmic difference using $W_{log} = (f_1(\theta, \phi))^{\beta}$ with $\beta = 0.5$, (c) the linear difference, and (d) the weighted linear difference using $W_{\text{lin}} = (f_1(\theta, \phi))^{-1}$. Note the different ranges of the vertical axes.

Based upon the previously defined differences, statistical measures of merit such as the mean difference and the standard deviation can be calculated. Here, the mean is given by

$$\mu = \frac{1}{N} \sum_{i=1}^{N} \Delta_i \tag{11}$$

and the standard deviation by

$$\sigma = \sqrt{\frac{1}{N-1} \sum_{i=1}^{N} (\Delta_i - \mu)^2} \tag{12}$$

where Δ_i represents one of the previously defined differences in each of the discrete points considered and N is the total number of points in which the difference is computed. An alternative statistical measure of merit is the Pth percentile δ_P of the absolute value of the difference. It is defined such that with a given probability P the absolute difference is below the value of δ_P. The Pth percentile can be determined from the calculated difference according to

$$P(|\Delta_i| \leq \delta_P) = \frac{N(|\Delta_i| \leq \delta_P)}{N} \tag{13}$$

where $N(|\Delta_i| \leq \delta_P)$ is the number of points in which the absolute value of the difference Δ_i is less than or equal to the Pth percentile δ_P. As an example, these statistical measures of merit have been calculated for the previously defined differences between the results DTU1 and DTU2 in the region $\theta \in [-180, 180]$ with $N = 3600$ and are presented in Table II. The Pth percentile as defined in (13) is strongly related to the cumulative distribution function (CDF) for the absolute difference, as it essentially represents a specific point on the curve described by the CDF [27]. Hence, instead of calculating the Pth percentile, it is possible to utilize the expression (13) to determine the CDF curve for the absolute difference. In Fig. 5 the CDF curves for the logarithmic difference of a few selected measurement results are shown. It is noted that the CDF for the

TABLE II
EXAMPLE OF STATISTICAL DATA FOR THE CONSIDERED DIFFERENCES (TO 3 DECIMALS)

Difference	Mean	STD	δ_{50}
Δ_{log} [dB]	−0.012	2.264	0.314
$\Delta_{w,log}$ [dB]	0.004	0.047	0.021
Δ_{lin}	0.000	0.001	0.000
$\Delta_{w,lin}$	−0.043	0.569	0.036

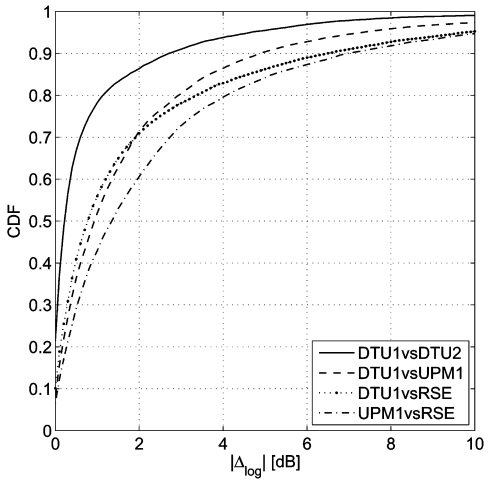

Fig. 5. The CDF for the logarithmic difference of various measured patterns.

absolute difference of two identical patterns would be a constant of one.

Aside from the statistical measures of merit, other measures of merit can be defined for expressing different specific characteristics of the differences between the examined patterns. One such measure is defined in the Feature Selective Validation (FSV) method [23], [24], which provides a measure of the degree of similarity of signals with particular focus on signals from electromagnetic measurements. Another measure of merit, specifically designed for comparison of the similarity of radiation patterns, has been proposed in [25] for multiband antennas. Also, recently an extensive discussion, based on simulated data, on quantitative measures for comparison of antenna patterns has been published in [26].

D. Methods For Comparisons

The weighting functions introduced in the definitions of the differences, (7) and (10), can be chosen in various ways to emphasize or de-emphasize certain properties of the differences, in certain parts of the pattern.

As an example, a continuous weighting function can be used to de-emphasize the influence from a noise floor in the measurement results. Based upon a known noise floor, e.g., $n = -60$ dB, three possible noise weighting functions, $W_{n,1}$, $W_{n,2}$, and $W_{n,3}$ are illustrated in Fig. 6.

The noise weighting functions in Fig. 6 all attribute a maximum weight at the maximum pattern level, while discarding differences at pattern levels below the noise floor, but they differ in between. Expressing the pattern function $f_1(\theta, \phi)$ in a logarithmic scale

$$D_1(\theta, \phi) = 20 \log_{10}(f_1(\theta, \phi)) \tag{14}$$

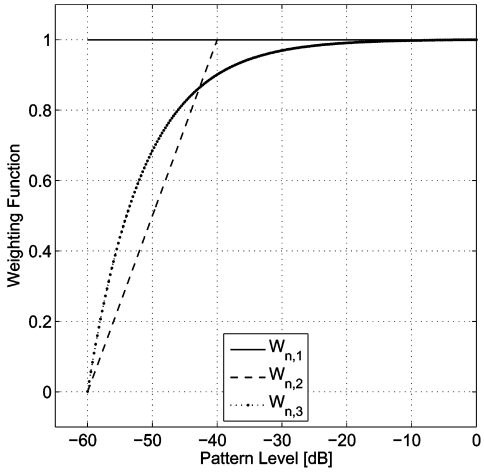

Fig. 6. Examples of weighting functions which can de-emphasize the influence on the difference from a noise floor in the measurement results.

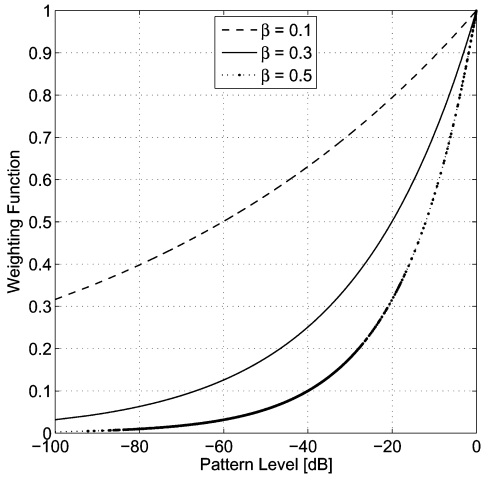

Fig. 7. Examples of the pattern weighting function W_p for different choices of β.

the noise weighting functions $W_{n,1}$, $W_{n,2}$, and $W_{n,3}$ can be expressed as follows (note that D_1 is in dB and a function of θ and ϕ)

$$W_{n,1} = \begin{cases} 1, & -60 \le D_1 \le 0 \\ \text{Discard}, & D_1 < -60 \end{cases} \tag{15}$$

$$W_{n,2} = \begin{cases} 1, & -40 \le D_1 \le 0 \\ \frac{D_1}{20} + 3, & -60 \le D_1 < -40 \\ \text{Discard}, & D_1 < -60 \end{cases} \tag{16}$$

$$W_{n,3} = \begin{cases} 1 + 10^{-60/20} - 10^{-60-D_1/20}, & -60 \le D_1 \le 0 \\ \text{Discard}, & D_1 < -60. \end{cases} \tag{17}$$

The noise weighting functions $W_{n,1}$ and $W_{n,2}$ are particularly simple examples. $W_{n,1}$ drops to zero, when the noise floor at -60 dB is reached. $W_{n,2}$ gives a linear drop in the interval -40 to -60 dB to suppress difference at low pattern levels approaching the noise floor. The final weighting function $W_{n,3}$ gives a weight, which is inversely proportional to the signal-to-noise ratio such that full weight is attributed to the difference at the peak pattern level, and then dropping to zero when approaching the noise floor.

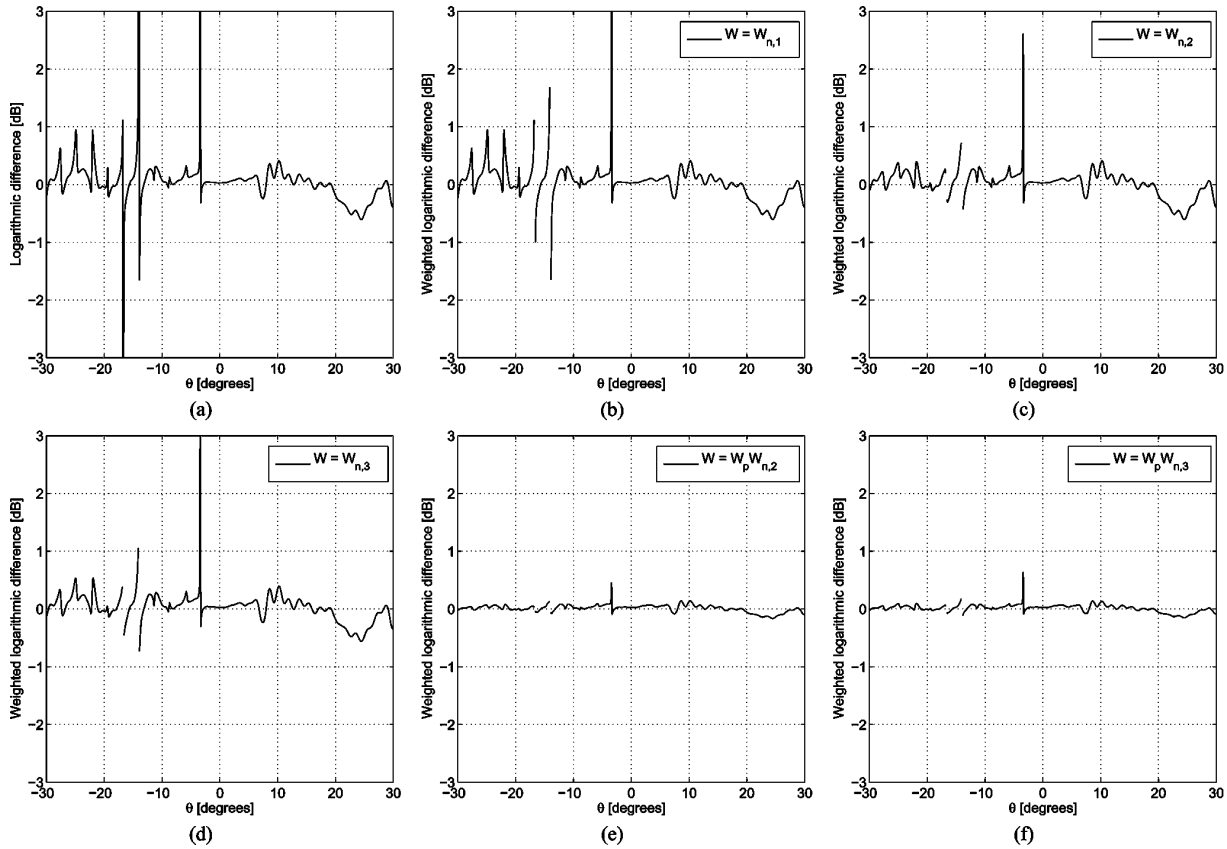

Fig. 8. The weighted logarithmic difference using various choices of the weighting functions. In (a) the logarithmic difference with no weighting is shown, in (b) $W = W_{n,1}$ is used, in (c) $W = W_{n,2}$ is used, in (d) $W = W_{n,3}$ is used, in (e) $W = W_p W_{n,2}$ is used, and in (f) $W = W_p W_{n,3}$ is used. The co-polar component of the DTU1 and DTU2 patterns at $\phi = 90^\circ$ in the optical coordinate system has been used in this example, and $\beta = 0.301$ has been used for the pattern weighting function W_p.

A so-called pattern weighting function can be introduced to emphasize certain parts of the pattern. This may be relevant in order to investigate other sources of inaccuracy than a noise floor or because of special requirements to the pattern. Such a pattern weighting function may be expressed as

$$W_p = \big(f(\theta, \phi)\big)^{\beta} \tag{18}$$

where the parameter β will determine the specific behavior of W_p. As an example, a choice of $\beta = -\log_{10}(1/2) = 0.301$ constitutes a weight for the difference that is halved for every 20 dB decrease in the pattern level. The pattern weighting function is illustrated in Fig. 7 for different choices of β. The combined weighting function will be the product of the noise and the pattern weighting functions

$$W = W_p W_n. \tag{19}$$

The effect of introducing a weighting of the logarithmic difference using the weighting functions presented here is illustrated in Fig. 8. It is seen from Fig. 8(b)–(d) that two peaks around $\theta = -15^\circ$ are significantly de-emphasized, while at other angles the difference remains to be almost the same. The pattern weighting function has much stronger effect, as it is seen from Fig. 8(e)–(f): the level of the difference is reduced and variation of the difference versus θ angle is equalized.

Due to the general nature of the defined weighting functions these can be used in the same manner for the linear difference as well.

Another method for comparing patterns and analyzing the difference is to separate the data into intervals around discrete pattern levels. This allows for investigations at specific pattern levels. However, by splitting the data into multiple intervals the extent of the comparisons also increases dramatically. While the investigations over full patterns lead to a single measure of merit, an investigation at several discrete levels leads to measures at each considered pattern level. In practice this involves defining an interval around selected discrete pattern levels, e.g., ± 1 dB or ± 3 dB intervals.

Examples of this method of comparison are investigations based on the mean, standard deviation and the Pth percentile, calculated in ± 3 dB intervals, which are presented in Fig. 9. It is seen that the values of all three measures of merit increase in general with the decreasing pattern level. However, this dependence is not quite monotonic: both mean and standard deviation show some oscillations.

In the following, it is investigated how these measures would behave in an ideal case, where each of the two measurements are influenced by only a constant noise floor. The logarithmic difference is thus

$$\Delta_{\log} = 20 \log_{10} \left(\frac{S + n_1}{S + n_2} \right) \tag{20}$$

where S is the true pattern and n_1 and n_2 are the noise in measurements 1 and 2, respectively. It is assumed that the noise in each measurement is a stochastic signal distributed uniformly between its extreme values centered around zero. The density functions are denoted by $g_1(n)$ and $g_2(n)$, respectively. The extreme value for the noise n_1 (n_2) is taken as $\pm nf_1$ $(\pm nf_2)$, where nf_1 (nf_2) is the noise floor; i.e., for a noise floor of -60 dB, the extreme values are $\pm 10^{-3}$. As a first step towards determining the density function of $\Delta_{\log}$ the stochastic variable X is now defined as

$$X = \frac{S + n_1}{S + n_2} \tag{21}$$

and the density function of X determined as [27]

$$g_X(x) = \int_{-\infty}^{\infty} g_1(xn) g_2(n) n \, dn. \tag{22}$$

The explicit form of $g_X(x)$ is rather lengthy and thus not reproduced here. The logarithmic difference is given from X as $\Delta_{\log} = 20 \log_{10}(X)$ and using [27, (2.2-11)] the density function of $\Delta_{\log}$ can be expressed from the density function of X as

$$g_\Delta(y) = \frac{\ln(10)}{20} g_X(10^{y/20}) 10^{y/20} \tag{23}$$

where y denotes the possible values of the logarithmic difference $\Delta_{\log}$. From this expression for the density function for the logarithmic difference the mean and standard deviation can be found as

$$\mu = \int_{-\infty}^{\infty} y g_\Delta(y) \, dy \tag{24}$$

$$\sigma = \sqrt{\int_{-\infty}^{\infty} (y - \mu)^2 g_\Delta(y) \, dy}, \tag{25}$$

and the Pth percentile of the absolute difference, δ_P, determined from

$$P(|\Delta_{\log}| \leq \delta_P) = \int_{-\delta_P}^{\delta_P} g_\Delta(y) \, dy. \tag{26}$$

In Figs. 10 and 11 these statistical measures are illustrated for different noise levels in pattern 1 and 2. For all three statistical measures an almost linear dependence on pattern level (in decibels) is noted. The mean, μ, is zero in the case of identical noise floors $(nf_1 = nf_2)$, and non-zero in case of different noise floors $(nf_1 \neq nf_2)$. In the latter case it is seen from a comparison of Figs. 10(a) and 11(a), that the level of the mean depends on both the level of the noise floors themselves and the difference between these, but the linear dependence on the pattern level remains the same for all noise floors. The standard deviation, σ has a level depending on both the level of the noise floors and their difference, and it converges towards a finite non-zero level for identical noise floors. This level depends on the common noise floor level. The 50th percentile of the absolute difference, δ_{50}, has a behavior which is qualitatively identical to that of the standard deviation. Comparing these statistical measures in Figs. 10 and 11 for an ideal case to those of Fig. 9 for a real case, it is concluded that the real measurements are influenced by other sources of inaccuracy than a constant noise floor. In particular it is noted that the mean in Fig. 9(a) has an oscillating behavior at high pattern levels and only at low pattern levels achieves an approximately linear behavior.

V. Comparisons

Measurement results from 8 facilities are available for the comparisons. In this section the gain and directivity as well as polarization characteristics are compared, and subsequently selected comparisons of the patterns are presented.

As stated in Section II the radiation patterns can be presented in either optical, mechanical, or electrical coordinate system. The exact mathematical transformation of the measurement results between these coordinate systems requires, e.g., a spherical wave expansion of the radiated field and the Euler angles relating the coordinate systems, but such information is not available at all facilities. Hence, the measurements from some facilities are only available in specific coordinate systems. The preferred coordinate system for the comparison campaign is the optical one, and in Figs. 12 and 13 the available patterns in this coordinate system are presented in the $\phi = 0°$ and $\phi = 90°$ planes, respectively. The patterns included are DTU1, DTU2, RSE, UPM1, UPM2, and UPC. This overview of the obtained patterns shows that there is generally a good agreement between most of the patterns, but noticeable differences can be observed in some regions, e.g., around $\theta = 25°$ in the $\phi = 90°$ plane.

The peak gain, peak directivity, loss, and on-axis gain measured by the participants are summarized in Table III. Generally, a very good agreement for the peak directivity can be observed, though the results from FTRD and UPC differ somewhat from the rest. For FTRD, a far-field facility, this is due to the fact that only a few ϕ-planes have been measured, while for UPC this may be due to the fact that no probe correction was applied. The peak gains are also seen to agree very well. Here, only DTU2 differs noticeably from the rest.

The on-axis polarization characteristics and peak location in the optical coordinate system are presented in Table IV. It can be noted that all values agree well for the tilt angle and axial ratio. The UPC values can be attributed to the fact that these results have not been probe corrected. The peak location is difficult to determine accurately since the main beam, while quite narrow in one direction, is wide in the other direction. This is reflected in the peak locations found by the participants, where the agreement in the θ coordinate is good, while the ϕ coordinate varies somewhat. In this particular case, since the absolute θ value is small, it is also useful to represent the peak location in (u, v) coordinate system defined as $u = \sin\theta \cos\phi$, $v = \sin\theta \sin\phi$, also shown in Table IV. In the detailed pattern comparisons presented below, the weighted logarithmic difference is employed. For this purpose a weighting function $W = W_n W_p$, including both noise weighting and pattern weighting is used. The noise weighting function $W_{n,3}$ (17) with a noise floor of $n = -60$ dB is used. The pattern weighting function W_p is given by (18) with $\beta = -\log_{10}(1/4) = 0.602$, which constitutes a weight reducing the difference by quarter for every 20 dB decrease in the pattern level.

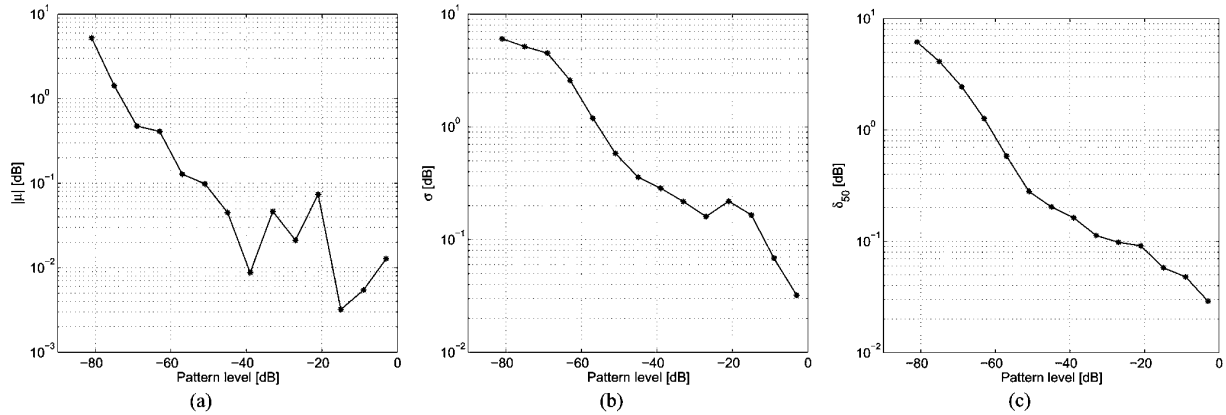

Fig. 9. Statistical measures for the logarithmic difference calculated for ± 3 dB intervals at discrete pattern levels. (a) shows the mean in each interval, (b) is the standard deviation, and (c) illustrates the 50th percentile δ_{50}. The co-polar component of the DTU1 and DTU2 patterns in the optical coordinate system has been used in this example.

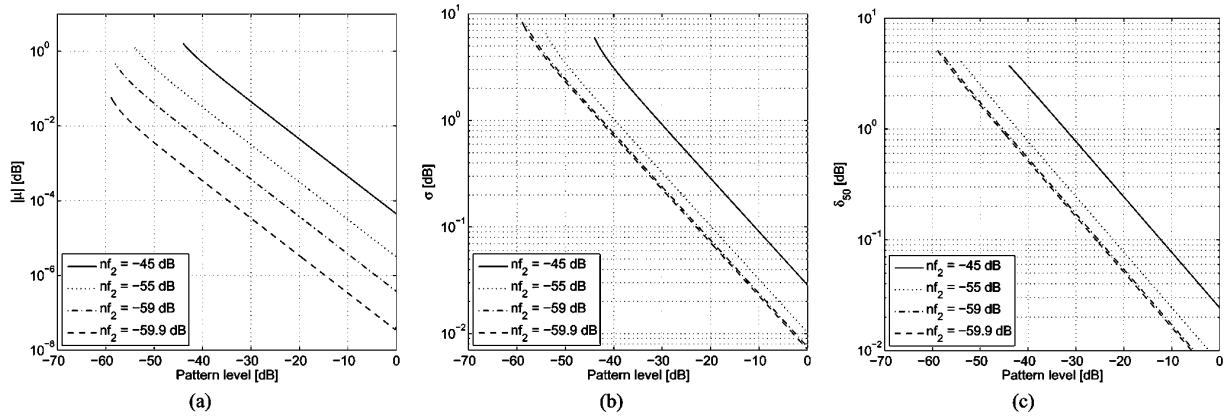

Fig. 10. Statistical measures for the logarithmic difference calculated for discrete intervals in the pattern level in the case of two ideal measurements influenced only by a noise floor. The magnitude of the noise in pattern 1 is $nf_1 = -60$ dB. (a) shows the mean difference, (b) is the standard deviation, and (c) illustrates the 50th percentile of the absolute difference δ_{50}.

A. Comparison of Two Spherical Near-Field Facilities

A total number of four spherical near-field measurement facilities participated in the comparison campaign. These were DTU, RSE, UPM1, and UPC. A comparison of the DTU2 and RSE measurement results in the optical coordinate system is presented here.

Fig. 14 shows the radiation patterns in the $\phi = 90°$ plane, which exhibit an agreement that is representative for the other planes as well. It is seen that the co-polar patterns agree very well except in the region around $\theta = 25°$, while the cross-polar patterns agree in shape, but disagree in level. The polarization characteristics presented in Table IV show a difference of about $0.7°$ in the tilt angle, which explains the difference in cross-polar level. This difference may be due to inaccuracies in alignment or inaccuracies in determination of the optical coordinate system with respect to the measurement coordinate system.

The weighted logarithmic difference is presented in Fig. 15 for the $\phi = 90°$ plane. It is seen that for the co-polar component the weighted logarithmic difference does not exceed 0.25 dB and generally stays below ± 0.1 dB, while for the cross-polar component it reaches -0.35 dB in the main beam region.

Based upon the weighted logarithmic difference the standard deviation and mean of the difference between the patterns have been determined. This has been done for the co- and cross polar components separately, and for both the full region ($\theta \leq 180°$) and for the boresight region ($\theta \leq 30°$). The results are presented in Table V. The smaller values for the full region are due to the use of the weighting functions; more points with larger differences are included, but these differences have a very small weight as they occur at low levels. Different values for co-polar and cross-polar components show that the latter is determined less accurately.

Figs. 16–18 show the discrete level mean, standard deviation, and 50th percentile, for the logarithmic difference. Comparing these to the theoretical curves in Fig. 10, it is clear that the patterns are affected by error sources that cannot be modelled by a constant noise floor. For example, it is seen that the curves for μ and σ are not monotonic, but oscillating with the pattern level. For both the mean and standard deviation, it is noted that the co- and cross-polar results show similar behavior for pattern levels below -45 dB, but different behavior for higher pattern levels.

B. Comparison of a Spherical Near-Field and a Far-Field Facility

A comparison of the measurement results from the FTRD far-field facility and the UPM1 spherical near-field facility is

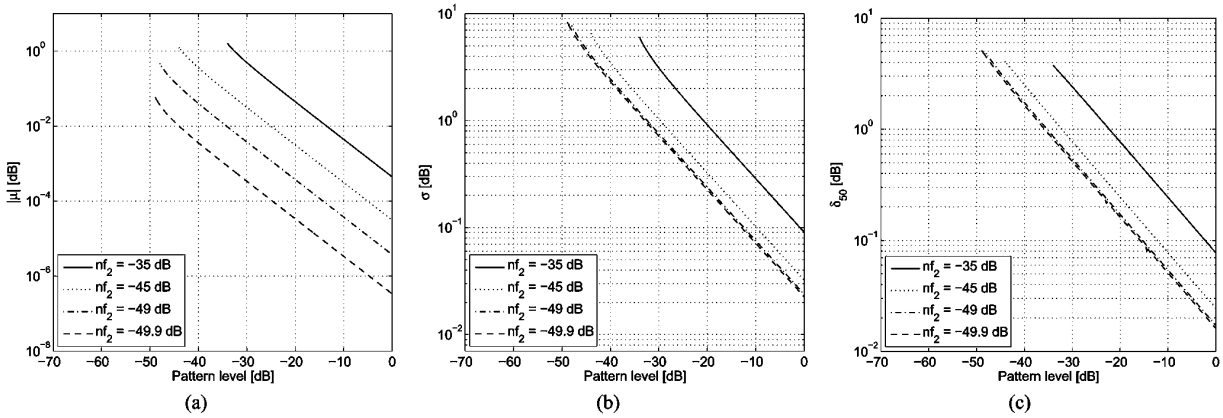

Fig. 11. Statistical measures for the logarithmic difference calculated for discrete intervals in the pattern level in the case of two ideal measurements influenced only by a noise floor. The magnitude of the noise in pattern 1 is $nf_1 = -50$ dB. (a) shows the mean difference, (b) is the standard deviation, and (c) illustrates the 50th percentile of the absolute difference δ_{50}.

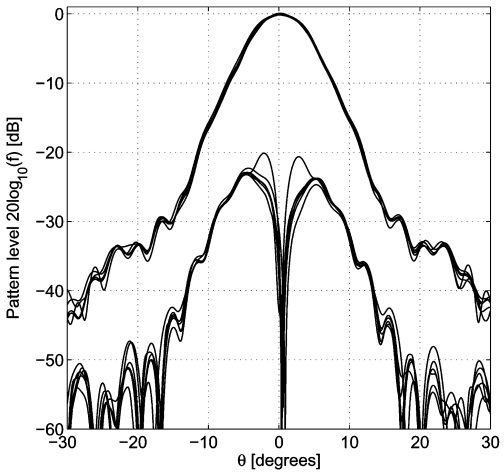

Fig. 12. All patterns available in the optical coordinate system, $\phi = 0°$ plane. The presented patterns are DTU1, DTU2, RSE, UPM1, UPM2, and UPC.

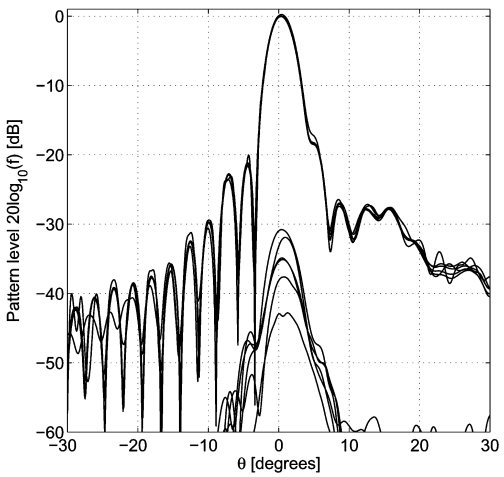

Fig. 13. All patterns available in the optical coordinate system, $\phi = 90°$ plane. The presented patterns are DTU1, DTU2, RSE, UPM1, UPM2, and UPC.

presented next. This comparison is performed in the electrical coordinate system.

Fig. 19 shows the radiation patterns in the $\phi = 90°$ plane, which exhibits an agreement that is representative for the other

TABLE III
THE PEAK DIRECTIVITY, PEAK GAIN, LOSS, AND ON-AXIS GAIN IN THE MECHANICAL COORDINATE SYSTEM (A DASH INDICATES THAT DATA IS NOT AVAILABLE)

Facility	Peak Directivity [dBi]	Peak Gain [dBi]	Loss [dB]	On-Axis Gain [dBi]
DTU1	30.71	30.35	0.36	30.33
DTU2	30.72	30.59	0.13	30.56
RSE	30.67	30.41	0.26	30.40
FTRD	31.1	30.4	0.7	–
UPM1	30.65	30.39	0.26	30.36
UPM2	–	30.38	–	30.33
UPM3	–	–	–	30.39
UPC	30.87	–	–	–
SMW	30.72	30.43	0.29	–

TABLE IV
THE ON-AXIS POLARIZATION CHARACTERISTICS AND PEAK LOCATION IN THE OPTICAL COORDINATE SYSTEM (A DASH INDICATES THAT DATA IS NOT AVAILABLE)

Facility	On-axis Tilt Angle [degrees]	On-axis Axial Ratio [dB]	Peak Location (θ, ϕ) [°]	Peak Location (u, v)
DTU1	-88.99	54.63	(0.44, 49.0)	(0.0050, 0.0058)
DTU2	-89.02	52.0	(0.54, 37.0)	(0.0075, 0.0057)
RSE	-88.36	53.3	(0.50, 42.3)	(0.0065, 0.0059)
FTRD	–	–	–	–
UPM1	-89.28	66.51	(0.40, 82.8)	(0.0009, 0.0069)
UPM2	–	–	(0.57, 90.0)	(0.0000, 0.0099)
UPM3	–	–	–	–
UPC	89.7	42	(0.45, 78.0)	(0.0016, 0.0077)
SMW	–	–	–	–

planes as well. Noticeable differences between the co-polar patterns are present in the region of side-lobes, while the cross polar patterns are very low and agree fairly well.

The weighted logarithmic difference is presented in Fig. 20 for the $\phi = 90°$ plane.

Based upon the weighted logarithmic difference the standard deviation and mean of the difference between the patterns have been determined. This has been done for the co- and cross polar components separately and has been done for the forward hemisphere region ($\theta \leq 90°$), and for the boresight region

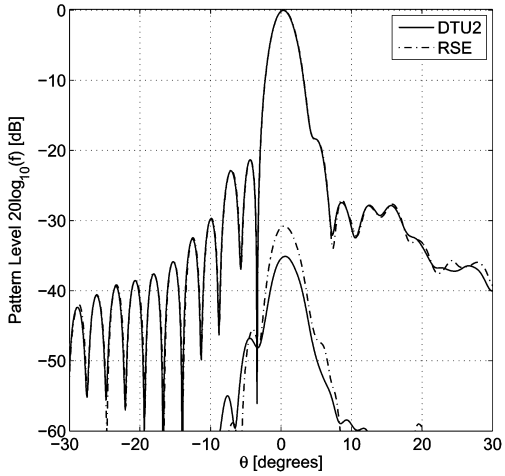

Fig. 14. The DTU2 and RSE radiation patterns in the $\phi = 90^\circ$ plane in the optical coordinate system.

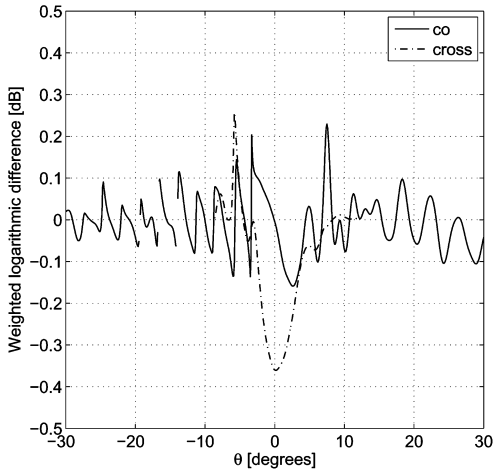

Fig. 15. Weighted logarithmic difference for DTU2 and RSE in the $\phi = 90^\circ$ plane.

TABLE V
STATISTICAL DATA FOR THE WEIGHTED LOGARITHMIC DIFFERENCE BETWEEN DTU2 AND RSE

	Mean	STD
co-polar ($\theta \leq 30^\circ$)	-0.011	0.056
cross-polar ($\theta \leq 30^\circ$)	-0.013	0.135
co-polar ($\theta \leq 180^\circ$)	-0.001	0.038
cross-polar ($\theta \leq 180^\circ$)	-0.001	0.066

($\theta \leq 30^\circ$). The results of this investigation are presented in Table VI. The values of the STD for the cross-polar component are smaller than for the co-polar component. This may be due to the weighting used in the calculation of the difference and the low level of the cross-polar pattern in the electrical coordinate system.

In Figs. 21–23 the discrete level mean, standard deviation, and 50th percentile, for the logarithmic difference, are presented. Comparing these to the theoretical curves in Fig. 10 it is again clear that the patterns are affected by error sources that cannot be modelled by a constant noise floor. The σ and δ_{50} curves are more linear in this case, compared to what was found in Figs. 17 and 18. Also, it can be noted that the co- and cross-polar results have more similar behavior for all pattern levels.

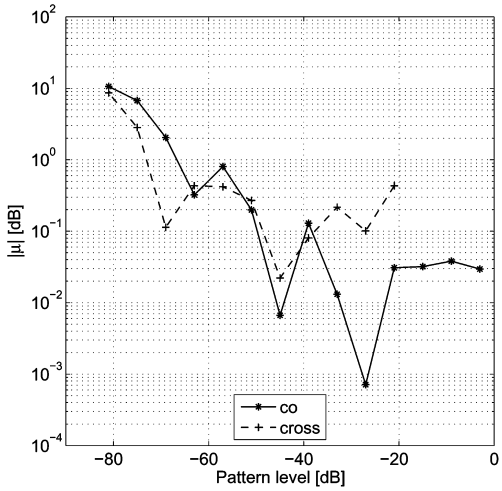

Fig. 16. Absolute value of the mean $|\mu|$ of the logarithmic difference in each ± 3 dB interval.

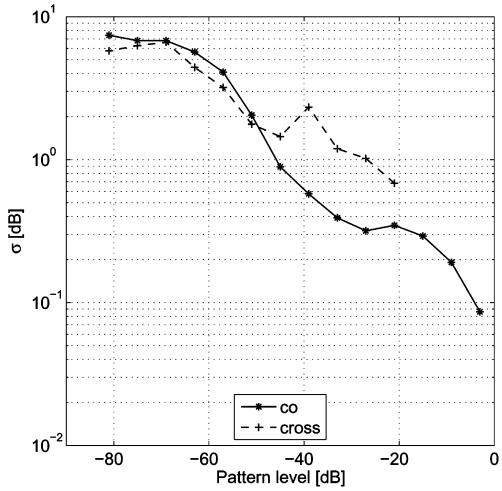

Fig. 17. Standard deviation σ of the logarithmic difference in each ± 3 dB interval.

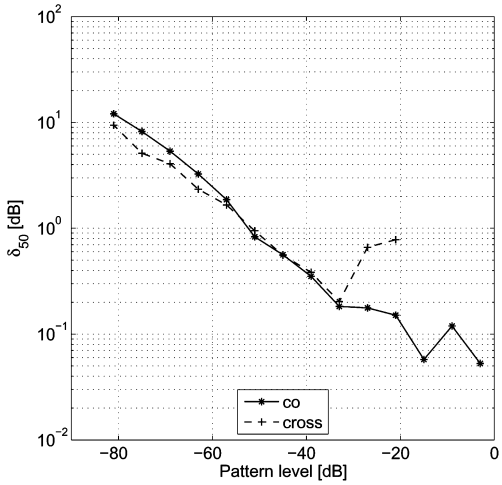

Fig. 18. 50th percentile, δ_{50}, of the absolute logarithmic difference in each ± 3 dB interval.

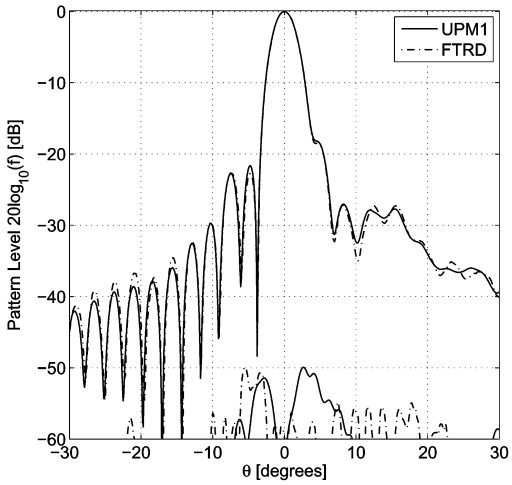

Fig. 19. The UPM1 and FTRD radiation patterns in the $\phi = 90^\circ$ plane in the electrical coordinate system.

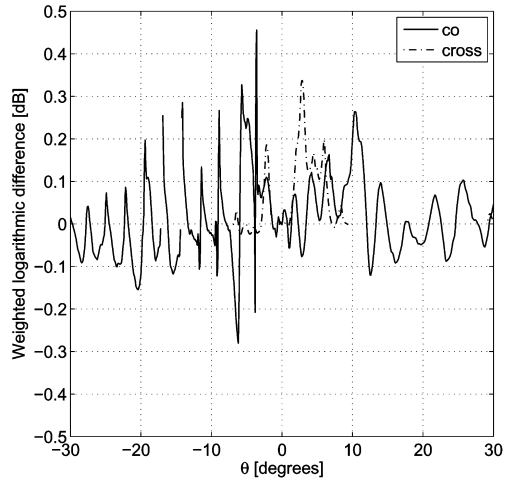

Fig. 20. Weighted logarithmic difference for UPM1 and FTRD in the $\phi = 90^\circ$ plane.

TABLE VI
STATISTICAL DATA FOR THE WEIGHTED LOGARITHMIC DIFFERENCE BETWEEN UPM1 AND FTRD

	Mean	STD
co-polar ($\theta \leq 30^\circ$)	0.013	0.124
cross-polar ($\theta \leq 30^\circ$)	0.028	0.074
co-polar ($\theta \leq 90^\circ$)	0.010	0.095
cross-polar ($\theta \leq 90^\circ$)	0.014	0.063

VI. CONCLUSION

This paper has documented a systematic comparison of eight antenna measurement facilities, based upon different measurement techniques and procedures, by the use of the DTU-ESA 12GHz Validation Standard Antenna. The comparison included four spherical near-field facilities, two compact ranges, a planar near-field facility, and a far-field facility.

Methods for doing comparisons of the measurement results have been discussed and examined through use on measurement results from the measurement campaign. Focus has been on comparisons of patterns and a number of methods for calculating the difference between patterns have been suggested. Furthermore, various quantitative measures of merit for determining the similarity of patterns have been proposed. Based on these measures, investigations were carried out for quantifying the pattern difference of the full patterns and for quantifying the pattern difference at discrete pattern levels.

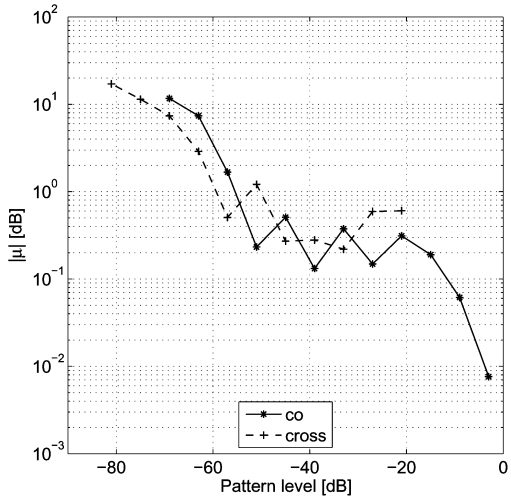

Fig. 21. Absolute value of the mean $|\mu|$ of the logarithmic difference in each ± 3 dB interval.

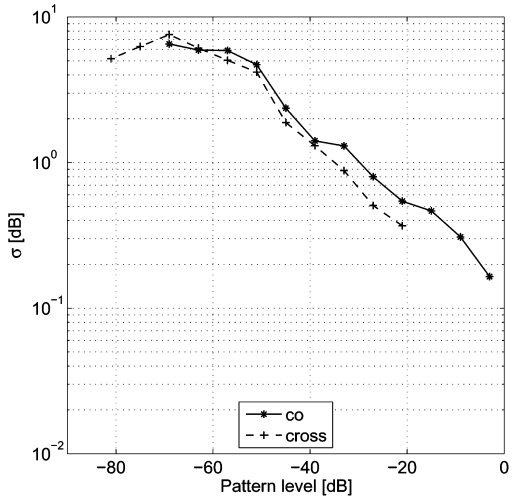

Fig. 22. Standard deviation σ of the logarithmic difference in each ± 3 dB interval.

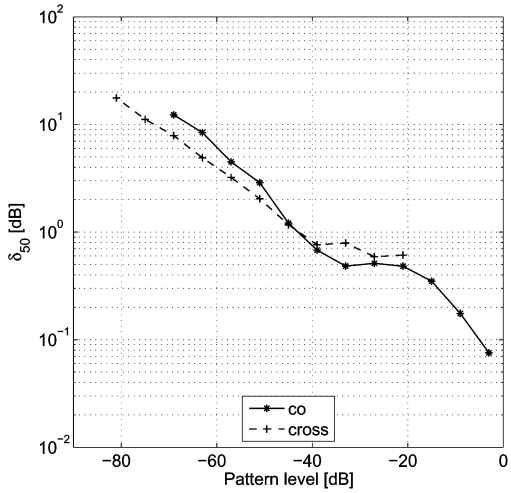

Fig. 23. 50th percentile, δ_{50}, of the absolute logarithmic difference in each ± 3 dB interval.

Comparisons of the measurement results have been presented. This includes a comparison of measured peak directivity and gain, antenna losses, peak location, polarization tilt angle, and axial ratio. Furthermore, two detailed comparisons of the measured patterns have been presented. The detailed comparisons were between two spherical near-field facilities, DTU2 and RSE, and between a spherical near-field and a far-field facility, UPM1 and FTRD, respectively.

The comparison was conducted within the EU Antenna Centre of Excellence with the primary purpose of obtaining experience and results that can serve to develop standards for validation of antenna measurement facilities. While facility comparisons constitute only one of several measures for facility validation, it is an important measure and, if conducted properly, it can provide very useful information on the accuracy of the participating antenna measurement facilities.

From the present investigatory comparison, that has focused on the radiation patterns, several significant conclusions have been reached.

First, it is important to employ a physically stable reference antenna with one, or more, well-defined coordinate systems. This ensures that differences between measurement results are actual differences between the measurements themselves—and not due to changes in the reference antenna or due to the use of different, or ill-defined, coordinate systems. The DTU-ESA VAST-12 antenna is one good reference antenna and there is obviously a need for a much wider range of such reference antennas.

Second, it is important to develop a detailed plan for the measurement campaign itself as well as the subsequent data processing of the measurement results. For the measurement campaign the Verification Test Plan ensures that the measured quantities and parameters are well-defined and that they are reported in a common data format. Since it was a purpose of the present comparison to investigate different procedures for data processing, a plan for this was not adopted beforehand here, but it is obviously of importance for the participating facilities to know how their measurement results will subsequently be processed and used.

Third, it would be advantageous that the reference antenna could be assigned a reference pattern. The determination of a reference pattern could be based on a combination of several measured patterns, where each pattern is weighted according to its accuracy estimate. Of course, this requires that accuracy estimates from different facilities be based on standard procedures. A reference pattern would obviously allow an effective benchmarking of the participating facilities.

Fourth, it is generally important for facility comparisons that standard procedures be developed for determination of accuracy estimates. Such procedures would be different for different measurement techniques and, for the same measurement technique, may be different for different measurements procedures.

Fifth, the use of weighting functions allows emphasizing particular interesting parts of the pattern and de-emphasizing e.g., differences close to the noise-floors of the two measurements. Here we have discussed and used different pattern and noise weighting functions.

Sixth, there are numerous possible statistical measures that can be invoked to characterize the difference between two patterns; here we have considered traditional measures such as mean, standard deviation, the Pth percentile, and the cumulative distribution function. While the latter is most appropriate for the full dynamic range of the patterns, the former three can also be applied to intervals at different levels. These statistical measures also form useful figures of merit for a condensed quantitative characterization of the difference between patterns.

Seventh, comparisons of measurement results potentially allow the identification of sources of inaccuracy in the measurements. This inverse problem requires that forward models be established to determine how one particular source of inaccuracy is reflected in the comparison. Here, we have presented a simple model that relates the levels of different noise floors to the statistical measures for the logarithmic difference between two patterns. From the actual comparisons included here it could thus be concluded that such noise floors are not the only source of inaccuracy for these particular measurements. This investigatory facility comparison has clarified a range of the many aspects involved in validation of antenna measurement facilities and provided useful information towards the development of standard validation procedures. The present comparison has focused on radiation pattern at a single frequency of 12 GHz and involved facilities of a generally high accuracy. Other comparisons have been conducted within the Antenna Centre of Excellence to cover many other antenna parameters as well as other and wider frequency bands [28]–[31].

ACKNOWLEDGMENT

The authors would like to thank the European Space Agency (ESA) for permitting the use of the DTU-ESA 12 GHz Validation Standard Antenna in this antenna measurement facility comparison campaign. Also, the authors would like to thank Jerzy Lemanczyk, ESA and anonymous reviewers for their comments and suggestions for this manuscript.

REFERENCES

[1] J. E. Hansen, Ed., *Spherical Near-Field Measurements*. London, U.K.: Peter Peregrinus Ltd., 1988.

[2] A. C. Newell, "Error analysis techniques for planar near-field measurements," *IEEE Trans. Antennas Propag.*, vol. AP-36, pp. 754–768, Jun. 1988.

[3] D. W. Hess, "An expanded approach to spherical near-field uncertainty analysis," in *Proc. AMTA* , Cleveland, OH, Nov. 2002, pp. 495–500.

[4] J. Lemanczyk and F. H. Larsen, "Comparison of near-field range results," *IEEE Trans. Antennas Propag.*, vol. AP-36, pp. 845–851, Jun. 1988.

[5] C. F. Stubenrauch, A. C. Newell, A. G. Repjar, K. MacReynolds, D. T. Tamura, F. H. Larsen, J. Lemanczyk, R. Behe, G. Portier, J. C. Zehren, H. Hollmann, J. D. Hunter, D. G. Gentle, and J. P. M. d. Vreede, "International intercomparison of horn gain at X-band," *IEEE Trans. Antennas Propag.*, vol. AP-44, pp. 1367–1374, Oct. 1996.

[6] D. G. Gentle, A. Beardmore, J. Achkar, J. Park, K. MacReynolds, and J. P. M. de Vreede, CCEM Key Comparison CCEM.RF-K3F (GT-RF 92-1). Measurement techniques and results of an intercomparison of horn antenna gain in IEC-R 320 at frequencies of 26.5, 33.0 and 40.0 GHz Nat. Phys. Lab., Teddington, U.K., 2003, NPL Rep. CETM 46.

[7] J. Lemanczyk and F. H. Larsen, Experimental Spherical Near Field Antenna Test Facility, Phase 3, Final Report Vol. III: An Intercomparison of Antenna Measurements Made At a Spherical Near Field Range (TUD), a Cylindrical Near Field Range (MBB) and a Compact Test Range (THE) Technical Univ. Denmark, Lyngby, Denmark, 1983, Tech. Rep. R282.

[8] J. Lemanczyk, An Intercomparison of Near Field Antenna Measurements Carried Out at TUD, MSS and BAe Tech. Univ. Denmark, Lyngby, Denmark, 1986, Tech. Rep. R323.

[9] J. Lemanczyk, Technical Assistance for the Design and Development of Antenna Test Range Validation Standardization. ESTEC CATR Intercomparison With the TUD-ESA Spherical Near Field Antenna Test Facility Tech. Univ. Denmark, Lyngby, Denmark, 1993, Tech. Rep. R557.
[10] J. Lemanczyk, An Intercomparison of Measurements Carried Out on the ERS-1 SAR Breadboard Antenna Panel at the Tech. Univ. Denmark and CASA, Spain Tech. Univ. Denmark, Lyngby, Denmark, 1995, Tech. Rep. R612.
[11] M. Dich and H. E. Gram, An Intercomparison of Measurements Carried out on the ERS-1 SAR Breadboard Antenna Panel at the Tech. Univ. Denmark and Alcatel Espace, France Tech. Univ. Denmark, Lyngby, Denmark, 1997, Tech. Rep. R667.
[12] J. Fordham and M. Scott, "Antenna pattern comparison between an outdoor cylindrical near-field test facility and an indoor spherical near-field test facility," *IEEE Antennas Propag. Mag.*, vol. 46, pp. 146–151, Jun. 2004.
[13] J. Lemanczyk, "Antenna standards and laboratories in Europe," *IEEE Trans. Antennas Propag.*, vol. AP-44, pp. 347–350, Apr. 1995.
[14] Antennas Virtual Centre of Excellence. Antenna Centre of Excellence 2006 [Online]. Available: http://www.antennasvce.org/
[15] J. E. Pallesen, S. Pivnenko, and O. Breinbjerg, EU Antenna Centre of Excellence WP 1.2-2: First Facility Comparison Campaign. Final Report Tech. Univ. Denmark, Lyngby, Denmark, 2006, Tech. Rep. R728.
[16] O. Breinbjerg, S. Pivnenko, M. Castañer, and C. Sabatier, "Antenna measurement facility comparison campaign within the European Antenna Centre of Excellence," in *Proc. IEEE Int. Symp. Antennas Propag.*, Washington DC, Jul. 2005, vol. 4A, pp. 85–88.
[17] J. E. Hansen, Definition, Design, Manufacture, Test and Use of a 12 GHz Validation Standard Antenna. Executive Summary Tech. Univ. Denmark, Lyngby, Denmark, 1997, Tech. Rep. R672.
[18] J. Lemanczyk, O. Breinbjerg, J. E. Hansen, and J. Heebøll, "Definition and design of a standard antenna for antenna test range validation," in *Proc. ICAP'91*, York, U.K., Apr. 1991, pp. 926–929.
[19] J. Lemanczyk, O. Breinbjerg, and R. Torres, "Antenna test range validation," in *Proc. AMTA'91*, Boulder, CO, Oct. 1991, pp. 9–17.
[20] R. Torres and O. Breinbjerg, "Development of a standard antenna for test range validation," presented at the 14th ESA Workshop Antenna Meas. ESTEC, Noordwijk, The Netherlands, May 1991.
[21] J. Lemanczyk, Technical Assistance for the Design and Development of Antenna Test Range Validation Standardization. The Verification Test Plan Tech. Univ. Denmark, Lyngby, Denmark, 1994, Tech. Rep. R595.
[22] A. C. Ludwig, "The definition of cross polarization," *IEEE Trans. Antennas Propag.*, vol. AP-21, no. 1, pp. 116–119, Jan. 1973.
[23] A. Martin, "Quantitative data validation (automated visual evaluations)," Ph.D. disertation, De Montfort Univ., Leicester, U.K, 1999.
[24] A. Duffy, A. J. M. Williams, T. M. Benson, and M. S. Woolfson, "Quantitative assessment of experimental repeatability," *Proc. Inst. Elect. Eng. Sci. Meas. Technol.*, vol. 145, no. 4, pp. 177–180, Jul. 1998.
[25] J. M. Ruis, M. C. Santos, and J. Parrón, "Figure of merit for multiband antennas," *IEEE Trans. Antennas Propag.*, vol. AP-51, pp. 3177–3180, Nov. 2003.
[26] J. McCormick, S. F. Gregson, and C. G. Parini, "Quantitative measures of comparison between antenna pattern data sets," *Proc. Inst. Elect. Eng. Microw. Antennas Propag.*, vol. 152, no. 6, pp. 539–550, Dec. 2005.
[27] P. Beckmann, *Probability in Communication Engineering*. New York: Harcourt, Brace and World, 1967.
[28] L. Foged, P. Garreau, O. Breinbjerg, S. Pivnenko, M. Castañer, and J. Zackrisson, "Facility comparison and evaluation using dual ridge horn," in *Proc. AMTA'05*, Newport, RI, Oct. 2005, pp. 161–165.
[29] J. Carlsson, "Benchmarking of facilities for small terminal antenna measurements," in *Proc. IEEE Int. Symp. Antennas Propag.*, Washington DC, Jul. 2005, vol. 4A, pp. 105–108.
[30] L. Foged, B. Bencivenga, O. Breinbjerg, S. Pivnenko, G. Di Massa, and M. Sierra-Castañer, "Measurement facility comparisons within the European Antenna Centre of Excellence," in *Proc. AMTA'07*, St. Louis, MO, Nov. 2007.
[31] L. Foged, O. Breinbjerg, S. Pivnenko, C. Sabatier, H. Eriksson, A. Alexandridis, M. C. Sierra, J. Zackrisson, and M. Boettcher, "Error calculation techniques and their application to the antenna measurement facility comparison within the European Antenna Centre of Excellence," presented at the 2nd Eur. Conf. Antennas Propag., Edinburgh, U.K., Nov. 2007.

Sergey Pivnenko (M'00) was born in Kharkiv, Ukraine, in 1973. He received the M.Sc. and Ph.D. degrees in electrical engineering from Karazin Kharkiv National University (KNU), Ukraine, in 1995 and 1999, respectively.

From 1998 to 2000, he was a Research Fellow at the Radiophysics Department, KNU. In 2000, he joined the Antennas and Electromagnetics Group, Department of Electrical Engineering, Technical University of Denmark, Lyngby, where he now works as Associate Professor and operates the DTU-ESA Spherical Near-Field Antenna Test Facility.

Since 2000, he participated to several research projects related to design, development and characterization of satellite antennas, development of new near-field probes and probe correction techniques for near-field antenna measurements. From 2004 to 2007, he was a Work Package Leader in the European Union network "Antenna Center of Excellence" where he was responsible for antenna measurement facility comparisons and participated to the other activities related to antenna measurements. His research interests include antenna measurement techniques, antenna analysis and design.

Janus E. Pallesen was born in Århus, Denmark, in 1979. He received the M.Sc. degree from the Technical University of Denmark, Lyngby, in 2005.

From 2005 to 2006, he was with the Department of Electrical Engineering, Technical University of Denmark as a Research Assistant. He is currently with Interactive Sports Games, Vedbæk, Denmark, as a Development Engineer working with monopulse radar systems.

Olav Breinbjerg (M'87) was born in Silkeborg, Denmark, on July 16, 1961. He received the M.Sc. and Ph.D. degrees in electrical engineering from the Technical University of Denmark (DTU), Lyngby, in 1987 and 1992, respectively.

Since 1991, he has been on the faculty of the Department of Electrical Engineering as Assistant Professor (1991–1995), Associate Professor (1995–2005), and Full Professor (since 2006). He is Head of the Electromagnetic Systems Group including the Antenna and Electromagnetics Group and the DTU-ESA Spherical Near-Field Antenna Test Facility. His research is generally in applied electromagnetics—and particularly in antennas, antenna measurements, computational techniques and scattering—for applications in wireless communication and sensing technologies. He is the author or coauthor of more than 35 journal papers, 100 conference papers, and 65 technical reports.

Prof. Breinbjerg received a U.S. Fulbright Research Award in 1995, the 2001 AEG Elektron Foundation's Award in recognition of his research in applied electromagnetics, and the 2003 DTU Student Union's Teacher of the Year Award for his course on electromagnetics.

Manuel Sierra Castañer (M'04) was born in Zaragoza, Spain, in 1970. He received the Engineer of Telecommunication degree in 1994 and the Ph.D. degree in 2000, both from the Technical University of Madrid (UPM), Madrid, Spain.

In 1997, he was with the University "Alfonso X" as an Assistant, and since 1998, at the Polytechnic University of Madrid as a Research Assistant, Assistant, and currently as an Associate professor. His current research interests are in planar antennas and antenna measurement systems.

Pablo Caballero Almena was born in Cabeza del Buey, Badajoz, Spain, in 1957. He received the Electronic Engineer degrees from the University of Comillas (ICAI), Spain.

He worked as a Laboratory Responsible in 1977 and since 1981 he is the Engineer responsible for the antenna measurements at the Technical University of Madrid (UPM), Madrid, Spain, working on multiple projects involved in measurement of satellite antennas, radomes, and radar cross section. He is also a Lecturer in Laboratory of Antennas at UPM.

Cristian Martínez Portas was born in Buenos Aires, Argentina, in 1977. He is currently working toward the the Computer Science Degree at the National University of Distance Education (UNED), Madrid, Spain.

Since 2002, he has worked as an Antenna Measurement Technician at the Technical University of Madrid (UPM). He has been measuring antennas, such as Amazon Hispasat Antennas or UMTS base station antennas and radomes for cellular telephony antennas. He is also the responsible for the computer network of the Radiation Laboratory of the UPM.

José Luis Besada Sanmartín was born in Pontevedra, Spain, in 1949. He received the Engineer of Telecommunication degree and the Ph.D. degree both from the Technical University of Madrid (UPM), Madrid, Spain, in 1971 and 1979, respectively.

In 1971, he joined the UPM where, since 1987, he is a Full Professor in the Signals, Systems and Radiocommunications Department. His current research interests are in reflector antennas design and manufacturing and antenna measurement systems.

Jordi Romeu was born in Barcelona, Spain, in 1962. He received the Ingeniero de Telecomunicación and Doctor Ingeniero de Telecomunicación from the Universitat Politècnica de Catalunya (UPC), Spain, in 1986 and 1991, respectively.

In 1985, he joined the Photonic and Electromagnetic Engineering Group, Signal Theory and Communications Department, UPC, where he is currently a Full Professor engaged in research in antenna near-field measurements, antenna diagnostics, and antenna design. He was Visiting Scholar at the Antenna Laboratory, University of California, Los Angeles, in 1999, on a NATO Scientific Program Scholarship, and in 2004 at University of California, Irvine. He holds several patents and has published 35 refereed papers in international journals and 50 conference proceedings.

Dr. Romeu was the Grand Prize Winner of the European IT Prize, awarded by the European Commission, for his contributions in the development of fractal antennas in 1998.

Sebastian Blanch (M'91) was born in Barcelona, Spain, in 1961. He received the Ingeniero and Doctor Ingeniero degrees in telecommunication engineering from the Polytechnic University of Catalonia (UPC), Barcelona, Spain, in 1989 and 1996, respectively.

In 1989, he joined the Electromagnetic and Photonics Engineering Group, Signal Theory and Communications Department. Currently, he is Associate Professor at UPC. His research interests are antenna near field measurements, antenna diagnostics, and antenna design.

José M. González-Arbesú was born in Barcelona, Spain, in 1967. He received the Ingeniero and Doctor Ingeniero degrees in telecommunication engineering, in 1992 and 2000, respectively, both from the Universitat Politècnica de Catalunya (UPC), Barcelona, Spain.

From 1994 to 2000, he was with the Signal Theory and Communications Department, Universidad de Zaragoza, Spain, where he was Lecturer. From 2000 to 2001, he was working for Tradia (telecommunications infrastructures and services operator) within the Radio Link Department as Radio Network Planning Engineer. Since 2002, he holds a research position with the Universitat Politècnica de Catalunya under the Ramón y Cajal tenure-track Programme. His research activities included antenna near-field measurements using infrared thermograms, performance evaluation of small fractal antennas, and, currently, antenna systems design integrated with high impedance surfaces.

Christian Sabatier (M'91) was born in Saint Yrieix La Perche, France, on September 4, 1959. He received the Ph.D. degree in microwaves and optical communications from the University of Limoges, France, in 1986.

After graduating, he joined the Antennas Department, France Telecom Research and Development, where he has worked on many activities: waveguide discontinuities, compact antennas for mobile phones, base station antennas, antennas for STENTOR and STELLAT satellites, multiband and UWB antennas. Measurements of antennas are also part of his interests.

Alain Calderone, photograph and biography not available at the time of publication

Gérard Portier, photograph and biography not available at the time of publication.

Håkan Eriksson (M'87) was born in Gothenburg, Sweden, on March 18, 1963. He received the M.Sc. degree in electrical engineering from Chalmers University of Technology (CTH), Gothenburg, in 1987.

He has since been with Saab Microwave Systems, formerly Ericsson Microwave Systems, where he is now Sr. Specialist in Antenna Measurement and Technical Leader for the ISO 17025 accredited Compact Antenna Test Range. He is currently a Member of the EU COST-IC0603 on Antenna Systems and Sensors. He was a Member of the EU Network of Excellence, Antenna Centre of Excellence, from 2004 to 2008. He is the author or coauthor of more than 20 journal papers or conference papers.

Dr. Eriksson is a member of the Antenna Measurement Techniques Association (AMTA).

Jan Zackrisson (M'02) was born in Gothenburg, Sweden, in 1957. He received the B.S. degree in electrical engineering in 1977. He has also studied master courses in physics, microwaves, antennas, space technology, economics and business administration between 1982 and 1996.

He joined Ericsson, Mölndal, Sweden, in 1978 where he worked with antennas until 1992. The work included design and test of satellite antennas as well as antennas for communication and radar applications. Since 1992, he has been with RUAG Aerospace Sweden (formerly Saab Ericsson Space), Gothenburg, Sweden where his current position is Senior Engineer responsible for antenna measurement techniques and for wide coverage antenna products.

Mr. Zackrisson is a member of the Antenna Measurement Techniques Association (AMTA).